(19) Bacon, G. E. "Neutron Diffraction", 3rd ed.; Oxford University Press: Oxford, 1975.
(20) de Gennes, P.-G "Scaling Concepts in Polymer Physics"; Cornell University Press: Ithaca, NY, 1979.
(21) Leibler, L.; Benoit, H. *Polymer* **1981**, *22*, 195.
(22) Ionescu, L.; Picot, C.; Dupplessix, R.; Duval, M.; Benoit, H.; Lingelser, J. P.; Gallot, Y. *J. Polym. Sci., Polym. Phys. Ed.* **1981**, *19*, 1033.
(23) de Gennes, P.-G. *J. Phys.* **1970**, *31*, 235.
(24) Boué, F.; Daoud, M.; Nierlich, M.; Williams, C.; Cotton, J. P.; Farnoux, B.; Jannik, G.; Benoit, H.; Dupplessix, R.; Picot, C. *Neutron Inelastic Scattering, Proc. Symp., 1977* **1978**, *1*, 563. Duplessix, R.; Cotton, J. P.; Benoit, H.; Picot, C. *Polymer* **1979**, *20*, 1181.
(25) Helfand, E.; Wasserman, Z. R. In "Developments in Block Copolymers"; Goodman, I., Ed.; Applied Science: London, 1982.
(26) Ramakrishnan, V. *J. Appl. Cryst.*, submitted.
(27) Stanley, H. E. "Introduction to Phase Transitions and Critical Phenomena"; Oxford University Press: Oxford, 1971.
(28) Whitmore, M. D.; Noolandi, J. *Macromolecules*, in press.
(29) Guinier, A.; Fournet, G. "Small-Angle Scattering of X-Rays"; Wiley: New York, 1955.
(30) Flory, P. J. "Principles of Polymer Chemistry"; Cornell University Press: Ithaca, NY, 1953.
(31) Herkt-Maetzky, C.; Shelton, J. *Phys. Rev. Lett.* **1983**, *51*, 896.
(32) Hadziioannou, G.; Stein, R.; Higgins, J. *Polym. Prepr. (Am. Chem. Soc., Div. Polym. Chem.)* **1983**, *24*, 213.
(33) Maconnachie, A.; Kambour, R. P.; White, D. M.; Rostami, S.; Walsh, D. J. *Macromolecules* **1984**, *17*, 2645.
(34) Sanchez, I. In "Polymer Blends"; Paul, D. R.; Newman, S., Eds.; Academic Press: New York, 1978; Vol. 1.
(35) Flory, P. J. *Discuss. Faraday Soc.* **1970**, *49*, 7.
(36) Bates, F. S.; Wignall, G. D.; Koehler, W. C. *Phys. Rev. Lett.*, in press.
(37) Rainville, E. D. "Special Functions"; Chelsea: New York, 1960.

Theory of Phase Equilibria in Block Copolymer–Homopolymer Blends

Mark Douglas Whitmore† and Jaan Noolandi*

Xerox Research Centre of Canada, 2660 Speakman Drive, Mississauga, Ontario, Canada L5K 2L1. *Received January 15, 1985*

ABSTRACT: The free energy of an inhomogeneous diblock copolymer–homopolymer blend is evaluated by using the functional integral formalism for multicomponent systems developed earlier. The advantage of this approach is that all important physical effects, such as polymer chain stretching, conformational entropy changes near an interface, enthalpic terms, etc., as well as the connectedness of the blocks of the copolymer, are automatically taken into account. In order to simplify the theory we calculate the inhomogeneous contribution to the free energy, as well as the polymer distribution functions, in a perturbation scheme (Landau–Ginzburg expansion), assuming that the density fluctuations of the components are small in comparison with their average values. This approach is valid near the spinodal for microphase separation and is less reliable as the inhomogeneous free-energy term grows in magnitude. For simplicity the ordered phase is assumed to have a lamellar structure, so that the third-order term in the expansion of the free energy vanishes. The temperature–composition phase diagrams for styrene–butadiene copolymer mixed with either polystyrene or polybutadiene homopolymer are calculated as an example for a series of chain lengths. The curvature of the phase boundaries near eutectic or critical points is discussed in detail. The assumption of a lamellar structure restricts the direct transition between the mesophase and the homogeneous phase to second order, resulting in the coalescence of some binodal lines in the phase diagrams. The maximum solubility of the homopolymer in the ordered phase is found to be large (up to 30% w/w) but to decrease rapidly as the homopolymer molecular weight is increased. The condition for homopolymer-induced mesophase formation is found to be $Z_H/Z_C \gtrsim {}^1/_4$ for a symmetric copolymer and a selective homopolymer with degrees of polymerization Z_C and Z_H, respectively. A computer program for evaluating the phase diagrams is available as supplementary material.

1. Introduction

Recent experimental work on diblock copolymer–homopolymer blends using small-angle X-ray and light-scattering techniques has given a great deal of information about their microstructure.[1,2] The equilibrium temperature–composition phase diagram shows a number of transitions between ordered and homogeneous phases, as well as different morphologies for the microdomains. When coupled with the results of other studies on block copolymers and their blends,[3-8] a picture of great diversity in the mechanical and structural properties of these "polymeric alloys" begins to emerge.

The purpose of this paper is to provide a theoretical basis for future realistic calculations of the equilibrium phase diagrams of block copolymer–homopolymer blends. In earlier work, we have formulated a general theory of multicomponent polymeric systems based on the functional integral formalism developed by Helfand for homopolymer interfaces and pure block copolymers.[9-11] This theory involves the solution of modified mean field diffusion equations for the polymer distribution functions. The connectedness of the blocks of the copolymer is included explicitly in the formalism, along with constraints that restrict density fluctuations and conserve the number of molecules. The derivation of the general free energy for the inhomogeneous system includes all important physical effects such as changes in the conformational entropy of the polymers in an interphase region, stretching of polymer chains throughout the microdomains, various configurational entropy terms corresponding to localization of homopolymers and block copolymers as well as block copolymer joints, and interaction terms between different chemical species. The expressions for the mean fields that occur in the diffusion equations for the distribution functions involve integrals of the polymer distribution functions, and in general these equations have to be solved numerically in a self-consistent scheme. This has been done for the case of homopolymer interfaces,[9] pure block copolymers,[10,11] block copolymers with a nonselective solvent,[12] and block copolymers at a demixed homopolymer interface.[13] In many cases the numerical work has served as a valuable guide to a deeper understanding of the

†Permanent address: Department of Physics, Memorial University of Newfoundland, St. John's, NF, Canada A1B 3X7.

0024-9297/85/2218-2486$01.50/0

multitude of physical effects that contribute to the unique properties of these systems.

For understanding the behavior near the transition temperature at which the homogeneous system begins to order, it has proven valuable to develop a perturbation approach (Landau–Ginzburg expansion) to calculate the inhomogeneous free energy by assuming that the density fluctuations of the components are small in comparison with their average values. This was first done for pure block copolymer systems by Leibler,[14] although his theory could not be generalized for blends. Recently a general perturbation expansion for inhomogeneous multicomponent blends has been given[15] which can readily be used to study the block copolymer–homopolymer system. The perturbation expansion is expected to be strictly valid only near the spinodal for microphase separation and will lead to semiquantitative results as the magnitude of the inhomogeneous free energy grows away from the spinodal. Nevertheless, the results of this calculation are so simple, with the density profiles given by cosine functions of a single wavevector at different amplitudes, that with little effort the model gives some feeling for the terrain of a complicated phase diagram. At some stage, however, a fully self-consistent calculation should be carried out to check the range of validity of the perturbation approach.[16]

In section 2 we outline the perturbation scheme used to evaluate the inhomogeneous free energy of a block copolymer–homopolymer blend. In particular we discuss the recently discovered phenomenon of homopolymer-induced mesophase formation[8,17] and give an analytic derivation of the critical homopolymer chain length relative to the (symmetric) copolymer chain length, $Z_H/Z_C \gtrsim {}^1/_4$, necessary for the effect to occur. Analytic results are also given for the ordering transition temperature of a slightly asymmetric copolymer with no homopolymer present. Throughout this paper we have assumed that the microdomains have lamellar structure so that the third-order terms in the Landau–Ginzburg expansion can be ignored. For asymmetric copolymers this is probably incorrect. For pure copolymer Leibler[14] has predicted that the ordered mesophase at the highest temperature is spherical and transforms through cylindrical to lamellar structures for lower temperatures, with a similar progression presumably taking place for copolymer–homopolymer blends. However, we felt it was important to gain some understanding of the simplest morphology before embarking on the larger venture of including transitions between different ordered structures. For the lamellar case only, we find regions in the phase diagram corresponding to a single homogeneous phase (H) and two homogeneous phases (HH), as well as the mesophase (M), mesophase–homogeneous mixtures (MH), and (tentatively) two mesophases (MM).

Section 3 deals with the phase diagrams of a series of copolymers and homopolymers of different chain lengths. For definiteness, we have chosen to present the calculations for styrene–butadiene copolymers mixed with either polystyrene or polybutadiene homopolymer. We give a discussion of the boundary curvature rule as applied to these diagrams, taking into account that the vanishing of the third-order term in the Landau–Ginzburg expansion of the free energy for lamellar microdomains immediately restricts the direct transition between the M and H phases to second order. This results in the coalescence of the two binodal lines, which would normally describe the first-order transition between the two phases, into a single line that is the spinodal for microphase separation.

A discussion of the results is given in section 4. Particularly interesting is the prediction of a large solubility of the homopolymer in the mesophase, up to 30% w/w for the cases we have investigated. In addition, at a given temperature the solubility of the homopolymer is found to drop rapidly as the chain length of the homopolymer is increased. These theoretical results appear to be in qualitative agreement with recent experimental results,[1,2] which were not obtained for a lamellar morphology, however. A computer program for calculating the phase diagrams of block copolymer–homopolymer blends, assuming lamellar ordered phases, is given as supplementary material to this paper.

2. Theory

In this paper we study blends of diblock copolymers with homopolymers that have the same chemical composition as one of the blocks of the copolymer. As in previous work, we determine the reduced free energy per unit volume, $f = F/(\rho_0 V k_B T)$, where F is the total free energy, V the volume, ρ_0 a reference number density, k_B the Boltzmann constant, and T the absolute temperature. We define the volume fractions

$$\phi_\kappa(\mathbf{x}) = \rho_\kappa(\mathbf{x})/\rho_{0\kappa} \tag{2-1}$$

in terms of the reduced densities, since we assume an incompressible system with no volume change upon mixing.[16] Here $\rho_{0\kappa}$ is the density of the pure material in monomer segments per unit volume. Using eq 2-1 we obviously have the relation

$$\sum_\kappa [\rho_\kappa(\mathbf{x})/\rho_{0\kappa}] = 1 \tag{2-2}$$

which will be used frequently in the later derivations. In order to treat compressible systems we may introduce the free volume as an additional component, as shown in ref 18, but in the present paper we ignore this complication. Hence the theory in its present form is incapable of describing phase-separation behavior near the so-called lower critical solution temperature, since this is an entropy-driven process related to the compressible nature of the blend.[19,20]

The reduced free energy of the inhomogeneous mixture is the sum of two contributions

$$f = f_h + \Delta f \tag{2-3}$$

where f_h is the Flory–Huggins free energy of the homogeneous system and Δf is the contribution from the inhomogeneity, calculated *relative* to the uniform system. The Flory–Huggins term is the standard form, which in our notation reads[21]

$$f_h = \sum_\kappa^C \phi_\kappa \mu_{0\kappa} + \frac{1}{2}\sum_{\kappa\lambda}^C \chi_{\kappa\lambda}\phi_\kappa\phi_\lambda + \sum_\kappa^C (\phi_\kappa/r_\kappa) \ln \phi_\kappa \tag{2-4}$$

where ϕ_κ is the overall volume fraction of component κ, and $r_\kappa = \rho_0 Z_\kappa \rho_{0\kappa}^{-1}$, Z_κ being the degree of polymerization. The chemical potential of the pure component is $\mu_{0\kappa}$, and $\chi_{\kappa\lambda}$ is the Flory–Huggins interaction parameter. In order to avoid confusion with the later formulas, we have used the "C" over the summation sign in eq 2-4 to indicate that the copolymer is to be treated as a single component. For the block copolymer C = AB we have

$$f_A + f_B = 1 \tag{2-5}$$

where

$$f_A = r_{CA}/r_C \qquad f_B = r_{CB}/r_C$$

and the density of the pure copolymer is defined by

$$\rho_{0C}^{-1} = Z_C^{-1}(Z_{CA}\rho_{0A}^{-1} + Z_{CB}\rho_{0B}^{-1}) \tag{2-6}$$

with $Z_C = Z_{CA} + Z_{CB}$.

The interaction parameter of the copolymer with the other components is given by

$$\chi_{C\kappa} = f_A\chi_{A\kappa} + f_B\chi_{B\kappa} - f_Af_B\chi_{AB} \quad (2\text{-}7)$$

and χ_{CC} vanishes, as required. As shown in ref 21, the inhomogeneous contribution to the free energy may be written

$$\Delta f = \frac{1}{2V}\sum_{\kappa\lambda}\int d^3x\, d^3y \chi_{\kappa\lambda}(\mathbf{x}-\mathbf{y})\psi_\kappa(\mathbf{x})\psi_\lambda(\mathbf{y}) - \frac{1}{V}\sum_\kappa \int d^3x\, \psi_\kappa(\mathbf{x})\omega_\kappa(\mathbf{x}) - \sum_\kappa^C \frac{\phi_\kappa}{r_\kappa} \ln (\mathcal{Q}_\kappa/V) \quad (2\text{-}8)$$

where $\psi_\kappa(\mathbf{x})$ is the deviation of the local volume fraction $\phi_\kappa(\mathbf{x})$ from the average volume fraction

$$\psi_\kappa(\mathbf{x}) = \phi_\kappa(\mathbf{x}) - \phi_\kappa \quad (2\text{-}9)$$

and $\omega_\kappa(\mathbf{x})$ is the mean field effective potential. The Flory–Huggins interaction parameter $\chi_{\kappa\lambda}$ is related to the corresponding nonlocal function by

$$\chi_{\kappa\lambda} = \int d^3x\, \chi_{\kappa\lambda}(\mathbf{x}) \quad (2\text{-}10)$$

and the absence of a "C" over a summation sign in eq 2-8 means that the different blocks A and B of a copolymer C = AB are to be treated as separate components.

The derivation and evaluation of eq 2-8 involve minimizing a general free-energy functional subject to the constraints of no volume change locally upon mixing of the components (eq 2-2) and a constant number of particles.[16] This procedure leads to a set of modified diffusion equations for the polymer distribution functions, $Q_\kappa(\mathbf{x},t|\mathbf{x}_0)$, which give the probability for t repeat units along the chain to start at $\mathbf{x}_0$ and end at $\mathbf{x}$ (here t is defined as a fraction of the total degree of polymerization Z_κ, ranging from 0 to 1)

$$(1/r_\kappa)(\partial/\partial t)Q_\kappa(\mathbf{x},t|\mathbf{x}_0) = \tfrac{1}{6}\hat{b}_\kappa^2\nabla^2 Q_\kappa(\mathbf{x},t|\mathbf{x}_0) - \omega_\kappa(\mathbf{x})Q_\kappa(\mathbf{x},t|\mathbf{x}_0) \quad (2\text{-}11)$$

where $\hat{b}_\kappa^2 = \rho_{0\kappa}b_\kappa^2/\rho_0$, b_κ being the Kuhn length, with the initial condition

$$Q_\kappa(\mathbf{x},0|\mathbf{x}_0) = \delta(\mathbf{x}-\mathbf{x}_0) \quad (2\text{-}12)$$

Equations 2-8 and 2-11 form a complicated set of nonlinear coupled integral–differential equations, which in general have to be solved self-consistently by numerical methods. To complete the circle of equations we also have expressions for the mean fields $\omega_\kappa(\mathbf{x})$ and an integral relation between the fundamental distribution function $Q_\kappa(\mathbf{x},t|\mathbf{x}_0)$ and the polymer volume fraction $\phi_\kappa(\mathbf{x})$

$$\phi_\kappa(\mathbf{x}) = (\tilde{N}_\kappa/\mathcal{Q}_\kappa\rho_0)\int_0^1 dt \int d^3x' \int d^3x_0\, Q_\kappa(\mathbf{x}',1-t|\mathbf{x})Q_\kappa(\mathbf{x},t|\mathbf{x}_0) \quad (2\text{-}13)$$

for homopolymers, where $\tilde{N}_\kappa$ is the number of polymer molecules, and

$$\mathcal{Q}_\kappa = \int d^3x\, d^3x_0\, Q_\kappa(\mathbf{x},1|\mathbf{x}_0) \quad (2\text{-}14)$$

Relations similar to eq 2-13 and 2-14 hold for the copolymer, taking into account the connectivity of blocks. Equation 2-13 has a simple interpretation, which is that the polymer density at the point $\mathbf{x}$ is proportional to the sum of all probabilities of having the chain ends located anywhere, with any fraction of the contour length passing through the point.

The expression for the mean field $\omega_\kappa(\mathbf{x})$ is given in terms of derivatives of the local inhomogeneous free-energy density and involves the fundamental distribution function through relations such as eq 2-13. The expression for the *total* inhomogeneous free energy, Δf, given by eq 2-8, can be evaluated once the mean field and polymer densities are known. Although the calculation of Δf is complicated, the interpretation of the various terms in eq 2-8 is relatively simple. The first term reduces to a Flory–Huggins type of expression for the enthalpy if a contact interaction potential is assumed for $\chi_{\kappa\lambda}(\mathbf{x}-\mathbf{y})$. The second term in eq 2-8 represents the change in the "turning-back" or conformational entropy of the polymer chains in the regions of inhomogeneity, and the last term accounts for the change in the combinatorial entropy of the polymers. This physical distinction between the second and third terms is not unique, however, because the mean field functions are defined only up to an additive constant, and it is sometimes convenient to choose this constant so that the last term in eq 2-8 vanishes.[13] In this case changes in both conformational and configurational entropies are accounted for in the second term of Δf.

In the present paper we do not seek a full self-consistent solution of eq 2-11, but assume that the inhomogeneity is weak, i.e., $|\psi_\kappa(\mathbf{x})/\phi_\kappa| \ll 1$, and utilize a perturbation expansion for $Q_\kappa(\mathbf{x},t|\mathbf{x}_0)$ as a power series in $\omega_\kappa(\mathbf{x})$.[15] This allows us to write Δf as a power series in $\omega_\kappa(\mathbf{x})$ and to eliminate $\omega_\kappa(\mathbf{x})$ in favor of $\psi_\kappa(\mathbf{x})$ through the minimization of the free energy with respect to the mean field function. The result is an expression for Δf that involves only deviations of the local polymer volume fractions from the overall average volume fractions. As pointed out in the earlier paper,[15] this approach is strictly valid only near the spinodal line and diminishes in accuracy as $\psi_\kappa(\mathbf{x})$ grows away from the spinodal. Nevertheless, the calculation is much simpler than determining the full self-consistent solution, and the results for the various phase diagrams are expected to be semiquantitatively correct.

Since the inhomogeneous structure of the block copolymer–homopolymer blends is expected to be periodic, it is convenient to work with the Fourier transforms of the density fluctuations and the fundamental distribution functions[15]

$$\tilde{\psi}_\kappa(\mathbf{k}) = \int d^3x\, \psi_\kappa(\mathbf{x})e^{-i\mathbf{k}\cdot\mathbf{x}} \quad (2\text{-}15)$$

$$\tilde{Q}_\kappa(\mathbf{k},t|\mathbf{k}_0) = \int d^3x\, d^3x_0\, Q_\kappa(\mathbf{x},t|\mathbf{x}_0)e^{-i(\mathbf{k}\cdot\mathbf{x}-\mathbf{k}_0\cdot\mathbf{x}_0)} \quad (2\text{-}16)$$

The solution of eq 2-11 for $\tilde{Q}_\kappa(\mathbf{k},t|\mathbf{k}_0)$ can then be written down to all orders in ω_κ, as shown explicitly in ref 15. Expanding out the ln term in eq 2-8 and minimizing the resulting expression for Δf_κ give a series for $\tilde{\psi}_\kappa(\mathbf{k})$ in terms of the mean field functions. Inverting this series and inserting the result back in the equation for Δf give the expansion for the inhomogeneous free energy in terms of the Fourier components of the density fluctuations

$$\Delta f = \frac{1}{2V}\tilde{\chi}_{ij}\tilde{\psi}_i\tilde{\psi}_j + \frac{1}{2V}\sum_\kappa^C \frac{1}{r_\kappa\phi_\kappa}[g^\kappa]_{ij}^{-1}\tilde{\psi}_i\tilde{\psi}_j - \frac{1}{6V}\sum_\kappa^C \frac{1}{r_\kappa\phi_\kappa^2}[g^\kappa]_{ip}^{-1}[g^\kappa]_{jq}^{-1}[g^\kappa]_{kr}^{-1}g_{pqr}\tilde{\psi}_i\tilde{\psi}_j\tilde{\psi}_k + \frac{1}{24V}\sum_\kappa^C \frac{1}{r_\kappa\phi_\kappa^3}[g^\kappa]_{ip}^{-1}[g^\kappa]_{jq}^{-1}[g^\kappa]_{kr}^{-1}[g^\kappa]_{ls}^{-1}\left(\frac{3}{V}g^\kappa_{pq}g^\kappa_{rs} + 3g^\kappa_{pqt}[g^\kappa]_{tu}^{-1}g^\kappa_{urs} - g^\kappa_{pqrs}\right)\tilde{\psi}_i\tilde{\psi}_j\tilde{\psi}_k\tilde{\psi}_l \quad (2\text{-}17)$$

up to fourth order in $\tilde{\psi}_i$. Here i stands for both the species index κ_i and the wave vector $\mathbf{k}_i$, $i \equiv (\kappa_i, \mathbf{k}_i)$, and summations as well as integrations over repeated subscripts are implied. However, the summation index does not apply to the index κ but only to i, j, etc. The various matrix coefficients in

eq 2-17 have been defined in the earlier publication. The equilibrium density fluctuations are then determined by minimization of the function given by eq 2-17.[15]

We first concentrate on the second-order term in the free energy in order to analyze the stability of the homogeneous system relative to small fluctuations in the polymer densities. The second-order term is

$$\Delta f_2 = \frac{1}{2V}\left(\tilde{\chi}_{ij}\tilde{\psi}_i\tilde{\psi}_j + \sum_{\kappa}^{C} \frac{1}{r_\kappa \phi_\kappa}[g^\kappa]_{ij}^{-1}\tilde{\psi}_i\tilde{\psi}_j \right) \quad (2\text{-}18)$$

Our system consists of a diblock copolymer AB and another component S, which we take to be a homopolymer. In this case we have obviously

$$\tilde{\psi}_S(\mathbf{k}) = -[\tilde{\psi}_A(\mathbf{k}) + \tilde{\psi}_B(\mathbf{k})] \quad (2\text{-}19)$$

and eq 2-18 becomes

$$\Delta f_2 = \frac{1}{2V}\int \frac{d^3k}{(2\pi)^3}[a(k)|\tilde{\psi}_A(\mathbf{k})|^2 + 2b(k)\tilde{\psi}_A(\mathbf{k})\tilde{\psi}_B(-\mathbf{k}) + c(k) \times |\tilde{\psi}_B(\mathbf{k})|^2] = \frac{1}{2V}\int \frac{d^3k}{(2\pi)^3}[\lambda_+(k)|u(\mathbf{k})|^2 + \lambda_-(k)|v(\mathbf{k})|^2] \quad (2\text{-}20)$$

where

$$a = g_{AA}^{-1}/(r_C\phi_C) + 1/(r_S\phi_S g_S) - 2\tilde{\chi}_{AS} \quad (2\text{-}21)$$

$$b = g_{AB}^{-1}/(r_C\phi_C) + 1/(r_S\phi_S g_S) + \tilde{\chi}_{AB} - \tilde{\chi}_{AS} - \tilde{\chi}_{BS} \quad (2\text{-}22)$$

$$c = g_{BB}^{-1}/(r_C\phi_C) + 1/(r_S\phi_S g_S) - 2\tilde{\chi}_{BS} \quad (2\text{-}23)$$

$$\lambda_\pm = (1/2)(c + a \pm \Delta) \quad (2\text{-}24)$$

$$\Delta = [(c - a)^2 + 4b^2]^{1/2} \quad (2\text{-}25)$$

$$u = [\mathrm{sgn}(b)(\Delta - c + a)^{1/2}\tilde{\psi}_A - (\Delta + c - a)^{1/2}\tilde{\psi}_B]/(2\Delta)^{1/2} \quad (2\text{-}26)$$

$$v = [\mathrm{sgn}(b)(\Delta + c - a)^{1/2}\tilde{\psi}_A - (\Delta - c + a)^{1/2}\tilde{\psi}_B]/(2\Delta)^{1/2} \quad (2\text{-}27)$$

In eq 2-21–27 the argument $\mathbf{k}$ has been suppressed, and in eq 2-21–23 $g_S = g_S(\mathbf{k},-\mathbf{k})$ is the Debye function, which is given in general by

$$g_\kappa(\mathbf{k},-\mathbf{k}) = 2(x - 1 + e^{-x})/x^2 \quad (2\text{-}28)$$

where $x = Z_\kappa b_\kappa^2 k^2/6$ for each component. g_{AA}^{-1} etc. are elements of the inverse of the matrix.

$$\begin{pmatrix} g_{AA} & g_{AB} \\ g_{BA} & g_{BB} \end{pmatrix} = \begin{pmatrix} f^2_A g_A(\mathbf{k},-\mathbf{k}) & f_A f_B g_A(\mathbf{k}) g_B(\mathbf{k}) \\ f_A f_B g_A(\mathbf{k}) g_B(\mathbf{k}) & f^2_B g_B(\mathbf{k},-\mathbf{k}) \end{pmatrix} \quad (2\text{-}29)$$

where

$$g_\kappa(\mathbf{k}) = (1 - e^{-x})/x \quad (2\text{-}30)$$

Noting that $\lambda_-(k) < \lambda_+(k)$ and referring back to eq 2-20, we see that a saddle-point instability develops when $\lambda_-(k) = 0$. Denoting the value of $k \neq 0$ that minimizes λ_- locally by k^*, the spinodal with respect to microphase separation is given by

$$\lambda_-(k^*) = 0 \quad (2\text{-}31)$$

where k^* is a function of the composition of the system as well as the various molecular weights and interaction parameters (and hence temperature). Away from the spinodal, we assume that the fluctuations are still described by a single Fourier component k^*, namely the one which minimizes λ_- for that composition and temperature. This approximation, which is discussed in ref 15, allows us to evaluate the third- and fourth-order terms in the expansion of the inhomogeneous free energy and to calculate the binodals for microphase separation. In this paper we concern ourselves only with the simplest microdomain structure, namely the lamellar case, for which the third-order term in the free energy vanishes. The equilibrium density profiles are then simply circular functions of different amplitudes

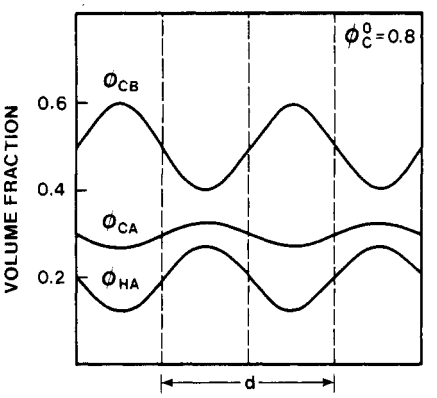

Figure 1. Density profiles of different components of a block copolymer–homopolymer system, calculated by assuming equal densities for the pure materials, with $f_A = Z_{CA}/Z_C = 3/8$, $f_B = Z_{CB}/Z_C = 5/8$, and the overall volume fraction of block copolymer given by $\phi_C^0 = 0.8$. The period of the microdomain structure is d. The densities of the different components fluctuate about their average values.

$$\psi_A(x) = \psi \cos k^* x \quad (2\text{-}32)$$

$$\psi_B(x) = \psi R(k^*) \cos k^* x \quad (2\text{-}33)$$

for the blocks of the copolymer, and

$$\psi_S(x) = -\psi[1 + R(k^*)] \cos k^* x \quad (2\text{-}34)$$

for the homopolymer component. The relative amplitude function $R(k^*)$ is given by

$$R(k^*) = -[\mathrm{sgn}\ b(k^*)]\left[\frac{\Delta(k^*) - c(k^*) + a(k^*)}{\Delta(k^*) + c(k^*) - a(k^*)}\right]^{1/2} \quad (2\text{-}35)$$

Figure 1 shows the results of a typical calculation for the concentration profiles of an asymmetric copolymer ($f_A = 3/8$, $f_B = 5/8$) mixed with homopolymer A ($\phi_{HA}^0 = 0.2$), assuming equal densities for the pure materials. The periodicity of the mesophase is d, and the densities of the different components oscillate about their average values.

In terms of the amplitude of the fluctuations, the expression for the free energy becomes

$$\Delta f = -\tfrac{1}{2}a\psi^2 + \tfrac{1}{4}\beta\psi^4 \quad (2\text{-}36)$$

where the expressions for a and β in terms of k^* and the appropriate matrix coefficients in eq 2-17 have been given in the earlier paper.[15] Minimizing of Δf with respect to ψ gives $\psi^2 = a/\beta$.

(a) Symmetric Block Copolymer with a Selective Solvent (Homopolymer). It has been shown earlier that for a symmetric block copolymer with a lamellar structure the condition $\chi_{AB}Z_C = 10.5$ must be satisfied for microphase separation to take place.[14] Here we are interested in calculating how the phase boundary between the homogeneous and microphase regions is shifted when small amounts of a highly selective solvent, such as a homopolymer corresponding to one of the blocks of the copolymer, is added to the system.

For the purposes of this calculation we take the densities of all pure components to be equal to the reference density, so that $r_C = Z_C$, $r_S = Z_H$. Substituting into the expression for λ_-, eq 2-24, and expanding all terms to first order in ϕ_H^0, we find that the value of λ_- at the minimum for $k = k^*$ is

$$\lambda_- = \frac{10.5}{Z_C} - \chi_{AB} + \left[\frac{10.5}{Z_C} - \frac{(\chi_{AS} - \chi_{BS})^2}{2} Z_H g_H\right]\phi_H^0 \quad (2\text{-}37)$$

where g_H is given by eq 2-30, with

$$x^* = \frac{Z_H b^2 k^{*2}}{6} = 3.78(Z_H/Z_C) \quad (2\text{-}38)$$

since $Z_C b^2 k^{*2} = 22.7$ for the pure copolymer. The boundary between the homogeneous and microphase regions corresponds to $\lambda_- = 0$, giving

$$\chi_{AB}Z_C = 10.5 + \left[10.5 - \frac{(\chi_{AS} - \chi_{BS})^2}{2} Z_H Z_C g_H\right]\phi_H^0 \quad (2\text{-}39)$$

For no change in the phase boundary to take place with the addition of small amounts of homopolymer the term in brackets in eq 2-39 must vanish. Taking the homopolymer to correspond to one of the copolymer blocks, this reduces to

$$1 - 5.25(Z_H/Z_C)g_H(x^*) = 0 \quad (2\text{-}40)$$

where we have used $\chi_{AS} = 0$, $\chi_{BS} = \chi_{AB}$, and $\chi_{AB}Z_C = 10.5$ near the phase boundary for the pure copolymer. Solving eq 2-40 with eq 2-38 gives

$$Z_C/Z_H = 3.9 \quad (2\text{-}41)$$

so that for $Z_H \simeq {}^1/_4 Z_C$ the slope of the phase boundary line with increasing ϕ_H^0 vanishes. It is easily verified from eq 2-39 that for $Z_H \ll {}^1/_4 Z_C$ the slope of the phase boundary is negative, while for $Z_H \gg {}^1/_4 Z_C$ the slope is positive. The results of calculations for various values of Z_H are shown in Figure 2. The crossover from negative to positive slope has a simple physical interpretation. For low temperatures, with $\chi_{AB}Z_C > 10.5$, the addition of a selective homopolymer of low molecular weight ($Z_H \ll {}^1/_4 Z_C$) eventually destabilizes the microphase because the loss of entropy in restricting the homopolymer to the compatible block region of the ordered phase becomes too large. In contrast, the entropy loss associated with localizing homopolymers of high molecular weight is negligible, and the gain in interaction energy in maintaining an ordered microphase, which provides a compatible environment for the selective homopolymer, is paramount. Hence, for high temperatures with $\chi_{AB}Z_C < 10.5$, the addition of small amounts of homopolymer of high molecular weight ($Z_H \ll {}^1/_4 Z_C$) induces the formation of a mesophase. This effect has been observed in the recent experiments by Cohen and Torradas.[8] It is also interesting to note that the slopes of the phase boundary lines shown in Figure 2 reach limiting values for very low or very high values of the ratio Z_C/Z_H.

(b) Asymmetric Block Copolymer. For the pure asymmetric block copolymer ($f_A \neq f_B$) λ_- is given by

$$\lambda_- = \frac{g_{AA}^{-1} + g_{BB}^{-1} - 2g_{AB}^{-1}}{2r_C} - \chi_{AB} \quad (2\text{-}42)$$

where g_{AA}^{-1}, etc. are elements of the inverse of the matrix given by eq 2-29. The condition for mesophase formation is $\lambda_-(k^*) = 0$, and for small deviations from a symmetric copolymer we find from an expansion of eq 2-42 in a power series

$$\chi_{AB}Z_C \simeq 10.5 + 21\left(\frac{Z_{CA} - Z_{CB}}{Z_C}\right)^2 + \ldots \quad (2\text{-}43)$$

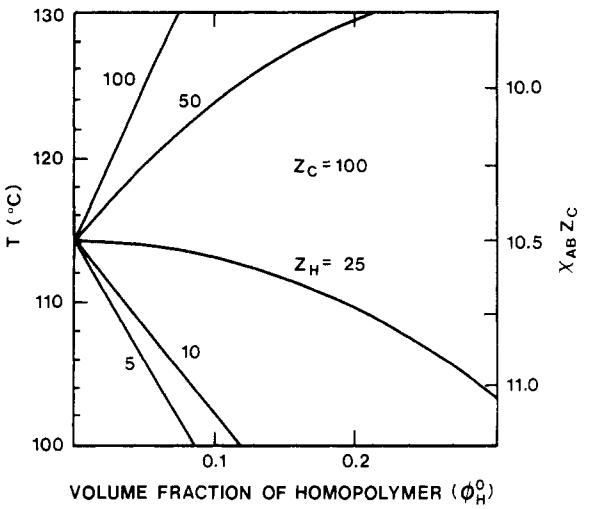

Figure 2. Phase boundary between the homogeneous phase and the mesophase for a homopolymer–block copolymer system with $Z_C = 100$ and different values of Z_H. The calculations assume equal densities for all components and equal block lengths for the copolymer. The right-hand scale ($\chi_{AB}Z_C$) has been converted to the left-hand scale (°C) by using the $\chi_{PS\text{-}PBD}$ parameter for polystyrene–polybutadiene (eq 3-8). The critical value for a change in slope at the point $\chi_{AB}Z_C = 10.5$ and $\phi_C^0 = 0$ is $Z_H/Z_C \simeq {}^1/_4$. For positive slope, the region to the left of the boundary is homogeneous and the region to the right is mesophase. For negative slope, the region to the left is mesophase and the region to the right is homogeneous.

for equal densities of all components. Generalizing eq 2-43 for different densities gives

$$\chi_{AB}Z_C(\rho_0/\rho_{0C}) = 10.5 + 21(f_A - f_B)^2 + \ldots \quad (2\text{-}44)$$

with ρ_0 the reference density for χ_{AB} and ρ_{0C} defined by eq 2-6. Comparison with numerical work for styrene–butadiene copolymer indicates that the first two terms in the expansion give the phase transition with an accuracy of within 1% for values of f_A up to 0.6. It should be kept in mind, however, that we have ignored the possibility of the formation of cylindrical or spherical microdomains, which have been predicted to have lower free energies for the asymmetric copolymer than the lamellar structure assumed here.

3. Phase Diagrams

(a) Temperature Dependence of the Binodals—Boundary Curvature Rule. In order to facilitate discussion of specific phase diagrams, we first derive some simple expressions for the changes in the binodals with temperature.[22] In general, let ϕ_1 and ϕ_2 represent the volume fractions of homopolymer at the binodal points in a binary polymer blend at temperature T. Expanding the free energy about the binodal point gives

$$f \simeq A(\phi_1,T) + B(\phi_1,T)(\phi - \phi_1) + (1/2)C(\phi_1,T)(\phi - \phi_1)^2 \quad (3\text{-}1)$$

for $\phi \simeq \phi_1$, with a similar expression for $\phi \simeq \phi_2$. The binodal points are joined by a single line of slope $B(\phi_1,T) = B(\phi_2,T)$, giving the relation

$$A(\phi_2,T) - A(\phi_1,T) = B(\phi_2,T)\phi_2 - B(\phi_1,T)\phi_1 \quad (3\text{-}2)$$

This is an implicit equation for the binodal points in terms of the free-energy function. Now consider a small temperature change δT and denote the new binodals by $\tilde{\phi}_1$ and $\tilde{\phi}_2$, where $\tilde{\phi}_1 = \phi_1 + \delta\phi_1$, etc. The free energy near ϕ_1 is then given by (still expanding about the first set of points ϕ_1 and ϕ_2)

$$f \simeq A(\phi_1,T+\delta T) + B(\phi_1,T+\delta T)(\phi - \phi_1) + (1/2)C(\phi_1,T+\delta T)(\phi - \phi_1)^2 \quad (3\text{-}3)$$

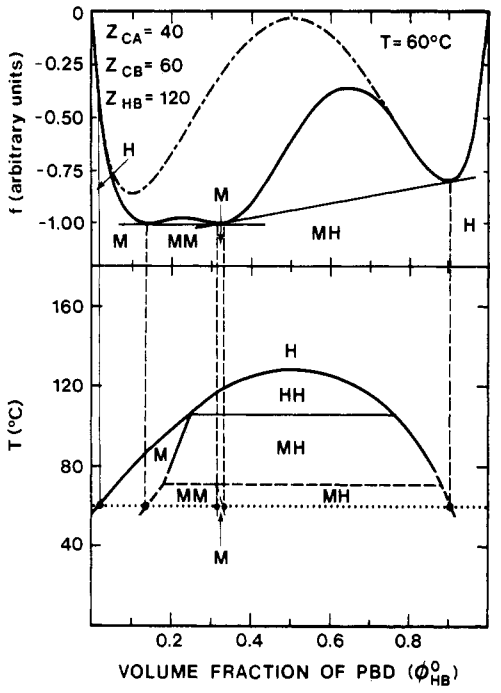

Figure 3. Phase diagram for styrene–butadiene block copolymer mixed with polybutadiene homopolymer for degrees of polymerization of the different components as marked on the diagram. The subscript A refers to polystyrene, and B to polybutadiene. The free-energy curves and binodal constructions for T = 60 °C are shown. The dot–dash line corresponds to the homogeneous free energy, and the solid line refers to the total free energy, including the inhomogeneous contribution. The different parts of the diagram are labeled H (homogeneous), HH (homogeneous–homogeneous), M (mesophase), MM (mesophase–mesophase), and MH (mesophase–homogeneous). The critical value of ϕ_{HB}^0 (called ϕ^* in the text) that marks the phase boundary between the mesophase and the homogeneous phase is denoted by the solid vertical line at the left of the diagram. The binodal points are indicated by dashed vertical lines. The lower part of the phase diagram is marked by dashed lines to indicate that the inhomogeneous free-energy term is large, and the weak perturbation theory which forms the basis of the calculation is of only semiquantitative significance here.

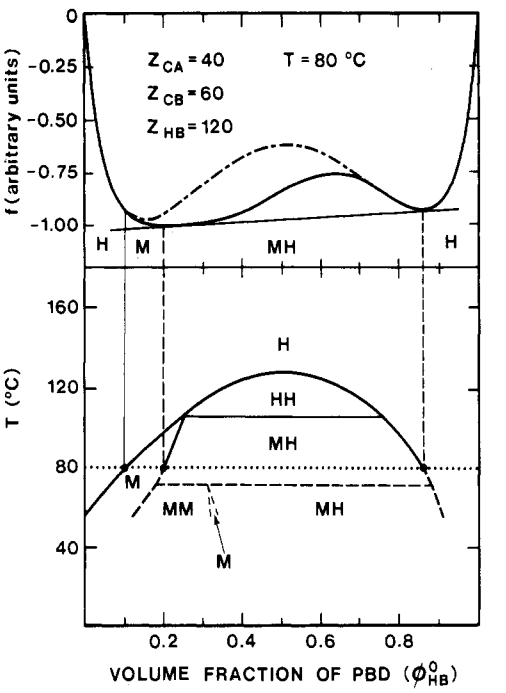

Figure 4. Same diagram as Figure 3, showing the free-energy curves and binodal constructions for T = 80 °C. Although the free energy has negative curvature near $\phi_{HB}^0 \simeq 0.3$, it lies above the tangent line joining the two binodal points, as shown.

and since the slopes at the new binodal points must be equal, we find the relation

$$B(\phi_1,T+\delta T) + C(\phi_1,T+\delta T)\delta\phi_1 = B(\phi_2,T+\delta T)C(\phi_2,T+\delta T)\delta\phi_2 \quad (3\text{-}4)$$

Linearizing this expression leads to

$$\delta T[B'(\phi_1,T) - B'(\phi_2,T)] + \delta\phi_1 C(\phi_1,T) - \delta\phi_2 C(\phi_2,T) = 0 \quad (3\text{-}5)$$

where the prime indicates the derivative with respect to temperature. Since the new binodal points must also be joined by a straight line, we find, similar to eq 3-2, the linearized equation

$$\delta T[A'(\phi_2,T) - A'(\phi_1,T) - \phi_2 B'(\phi_2,T) + \phi_1 B'(\phi_1,T)] - \delta\phi_2\phi_2 C(\phi_2,T) + \delta\phi_1\phi_1 C(\phi_1,T) = 0 \quad (3\text{-}6)$$

Using eq 3-5 to eliminate $\delta\phi_1$, we are able to determine how the binodal point varies with temperature,

$$\frac{\delta\phi_2}{\delta T} = \left[\frac{A'(\phi_2,T) - A'(\phi_1,T)}{\phi_2 - \phi_1} - B'(\phi_2,T)\right] C(\phi_2,T)^{-1} \quad (3\text{-}7)$$

with a similar expression for $\delta\phi_1/\delta T$, obtained by interchanging the subscripts 2 and 1 in eq 3-7. Later we will make extensive use of eq 3-7 for the block copolymer–homopolymer system, in particular for analyzing the curvature of the phase boundaries near coexistence temperatures.

(b) Block Copolymer–Homopolymer Blends. For definiteness, we consider a system of styrene–butadiene block copolymer mixed with either polystyrene or polybutadiene homopolymer. The Kuhn lengths are b_{PS} = 7.1 Å for polystyrene and b_{PBD} = 6.8 Å for polybutadiene,[23] and the temperature dependence of the corresponding densities are taken from ref 23 and 24. The interaction parameter is taken to be[25]

$$\chi_{PS\text{-}PBD} = -0.0835 + 73/T \quad (3\text{-}8)$$

where T is the temperature in kelvin and the polystyrene density is used for reference.

Figures 3–6 focus on one specific phase diagram for an asymmetric block copolymer of styrene–butadiene with a fixed molecular weight of the polybutadiene homopolymer. The series of diagrams displays the free energies and binodal constructions for different temperatures as a function of the volume fraction of homopolymer.

Following the general scheme outlined in section 2, we find that the inhomogeneous free energy, Δf, which is responsible for microphase formation, is negative over some regions of the phase diagram. A number of different cases arise. For the diagram shown in Figure 3, we have $\Delta f = 0$ for ϕ_{HB}^0 less than a critical value that we label ϕ^*, which is near the left binodal point, and $\Delta f < 0$ for $\phi_{HB}^0 > \phi^*$ until Δf vanishes again near the right binodal point. The solid line in the upper panel of the figures denotes the total free energy, including the inhomogeneous part, while the dot–dash line indicates the contribution from the homogeneous free energy alone. The difference is Δf.

Near the critical volume fraction ϕ^*, the inhomogeneous free energy has the expansion

$$\Delta f \simeq -\frac{\epsilon}{2}(\phi_{HB}^0 - \phi^*)^2 \qquad \phi \gtrsim \phi^* \quad (3\text{-}9)$$

$$\Delta f = 0 \qquad \phi < \phi^*$$

where $\epsilon(T)$ is a coefficient that in general depends on the different parameters of the system. Neither ϵ nor ϕ^* can be determined analytically for the asymmetric block co-

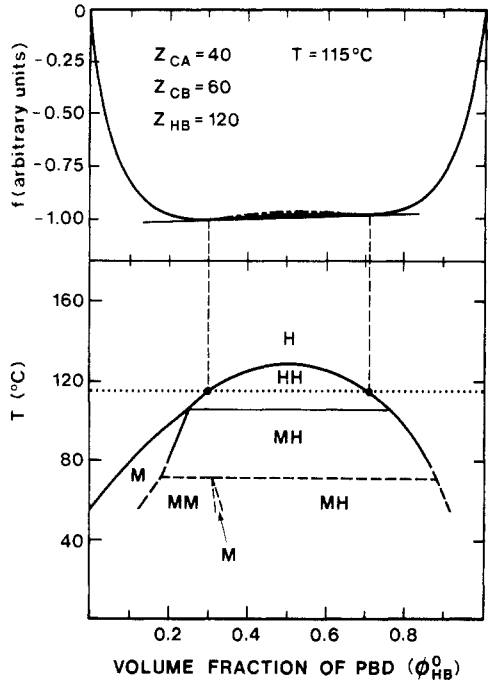

Figure 5. Same diagram as Figure 3, showing the free-energy curves and binodal constructions for $T = 115$ °C.

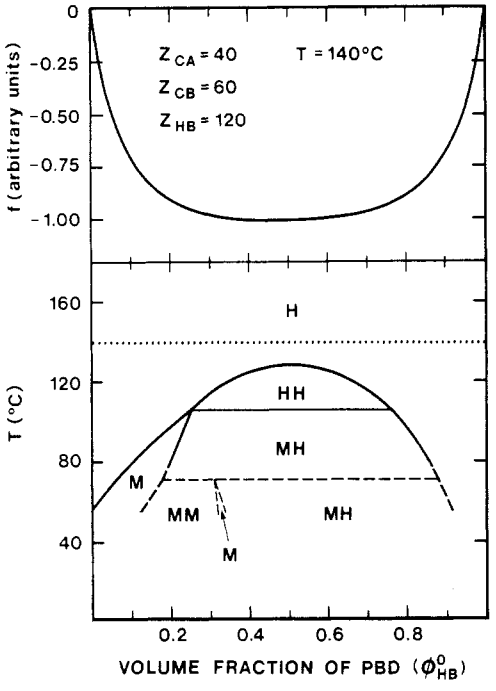

Figure 6. Same diagram as Figure 3, showing the free-energy curve for $T = 140$ °C.

polymer with a selective solvent. The absence of the linear term in eq 3-9 is significant and is related to the fact that we have allows for the formation of only lamellar mesophases. As we discuss later, this means that only a *second-order* transition can take place between the homogeneous phase and the ordered mesophase. The critical volume fraction ϕ^* is a smooth function of temperature and forms the boundary between the H and M phases at the left of the phase diagram. Eventually, as the temperature is raised, ϕ^* coincides with the binodal point ϕ_1 for a critical temperature $T = T_C$. For $T > T_C$ (Figure 5), $\phi^* > \phi_1$, and phase separation into two homogeneous phases takes place, with no microdomains present. As the temperature is raised further (Figure 6), the second derivative of the free energy remains positive and no phase separation occurs.

In order to understand the structure of the diagram near the eutectic point where two homogeneous phases and the mesophase coexist, we make use of eq 3-7 and 3-9 to determine the slopes of the binodals for $T \simeq T_C$. If the coefficients in the expansion of the free energy, eq 3-1, for the homogeneous blend are denoted by $\tilde{A}(\phi_1,T)$, etc., we have, expanding about the fixed binodal points ϕ_1 and ϕ_2 obtained for $T = T_C$,

$$f = \tilde{A}(\phi_1,T) + \tilde{B}(\phi_1,T)(\phi - \phi_1) + (1/2)\tilde{C}(\phi_1,T)(\phi - \phi_1)^2 \tag{3-10}$$

for $\phi \leq \phi^*$ and $T \simeq T_C$. Note that although ϕ_1 and ϕ^* coincide at $T = T_C$, by definition, the changes with temperature of these quantities are in general different. For $\phi > \phi^*$, the free energy includes the inhomogeneous contribution

$$f = \tilde{A}(\phi_1,T) - \frac{\epsilon}{2}(\phi_1 - \phi^*)^2 + [\tilde{B}(\phi_1,T) - \epsilon(\phi_1 - \phi^*)] \times (\phi - \phi_1) + (1/2)[\tilde{C}(\phi_1,T) - \epsilon](\phi - \phi_1)^2 \tag{3-11}$$

and near the other binodal point we have, for $\phi \simeq \phi_2$,

$$f = \tilde{A}(\phi_2,T) + \tilde{B}(\phi_2,T)(\phi - \phi_2) + (1/2)\tilde{C}(\phi_2,T)(\phi - \phi_2)^2 \tag{3-12}$$

The change in the binodal point ϕ_1 for $T < T_C$, for which $\phi_1 > \phi^*$, is obtained by using eq 3-11 and the expression analogous to eq 3-7

$$\lim_{T\to T_C^-} \frac{\delta\phi_1}{\delta T} = \left[\frac{\tilde{A}'(\phi_1,T_C) - \tilde{A}'(\phi_2,T_C)}{\phi_1 - \phi_2} - \tilde{B}'(\phi_1,T_C) - \epsilon(T_C)\frac{\partial\phi^*}{\partial T}\bigg|_{T=T_C} \right][\tilde{C}(\phi_1,T_C) - \epsilon(T_C)]^{-1} \tag{3-13}$$

and above T_C we have, using eq 3-10

$$\lim_{T\to T_C^+} \frac{\delta\phi_1}{\delta T} = \left[\frac{\tilde{A}'(\phi_1,T_C) - \tilde{A}'(\phi_2,T_C)}{\phi_1 - \phi_2} - \tilde{B}'(\phi_1,T_C) \right]\tilde{C}(\phi_1,T_C)^{-1} \tag{3-14}$$

Thus the slopes of the binodals are in general different above and below T_C, as shown in Figure 3. Note that the slopes in the diagram correspond to the inverse of eq 3-13 and 3-14. In fact, the numerator in eq 3-13 can sometimes vanish, giving rise to an infinite slope below T_C, as can be seen from one of the later phase diagrams (Figure 12). It can be easily shown from eq 3-7 that the variation in ϕ_2 with temperature leads to

$$\lim_{T\to T_C^+} \frac{\delta\phi_2}{\delta T} = \lim_{T\to T_C^-} \frac{\delta\phi_2}{\delta T} \tag{3-15}$$

so that there is *no* change in the slope of the binodal at $T = T_C$ near the *right* side of the phase diagram in Figure 3.

The physical significance of some of the features has been discussed in section 2 and in earlier papers.[13,15] Figure 3 shows the free-energy curves for $T = 60$ °C. At this temperature the magnitude of the inhomogeneous free energy and the amplitudes of the density variations are large, and the diagram has only a semiquantitative significance. Hence some of the boundaries between the different phases are indicated by dashed lines in this region. Beginning with a homogeneous system, induced

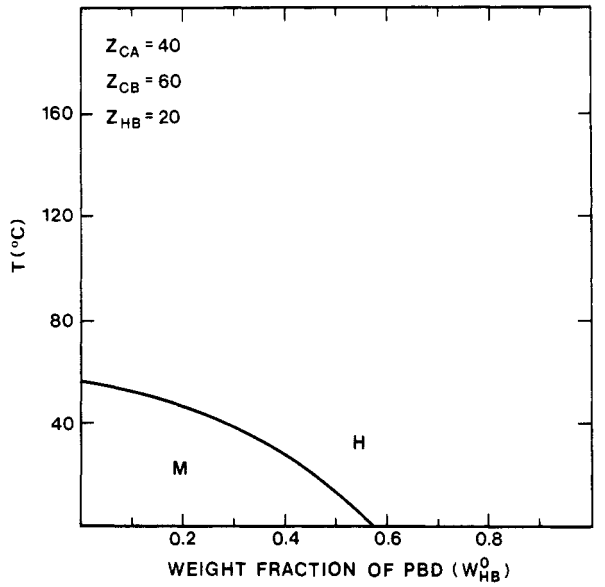

Figure 7. Phase diagram for a blend of polybutadiene homopolymer with styrene–butadiene block copolymer for the degrees of polymerization of the different components as indicated on the diagram. The subscript A refers to polystyrene, and B to polybutadiene. The different parts of the diagram are labeled M, H, etc., which refers to the different phases such as mesophase, homogeneous, etc. in the same way as in Figure 3. Note that the horizontal axis refers to weight fraction of polybutadiene (W_{HB}^0).

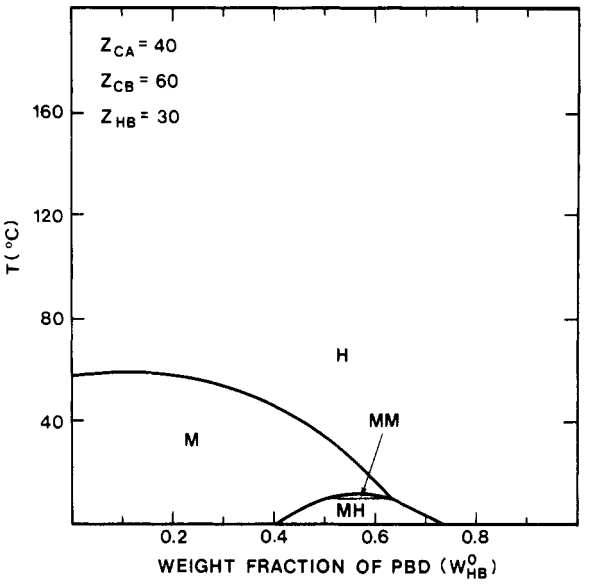

Figure 8. Phase diagram for a blend of polybutadiene homopolymer with styrene–butadiene block copolymer, as in Figure 7, but with an increased degree of polymerization for the butadiene homopolymer.

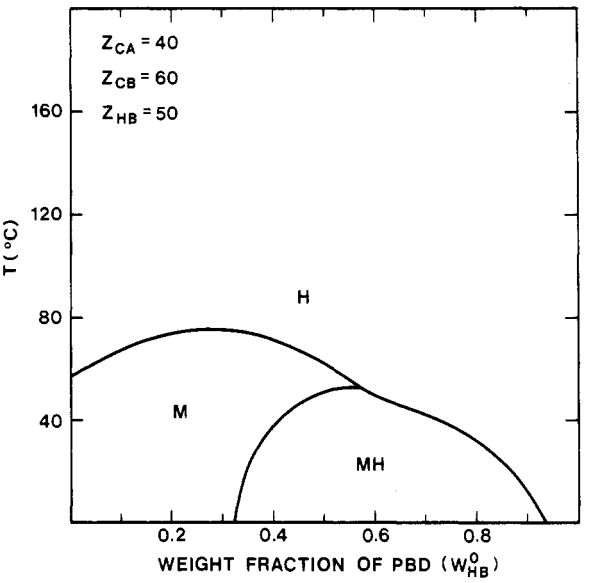

Figure 9. Phase diagram for a blend of polybutadiene homopolymer with styrene–butadiene block copolymer, as in Figure 8, but with an increased degree of polymerization for the butadiene homopolymer.

mesophase formation soon takes place as polybutadiene homopolymer is added to styrene–butadiene block copolymer at T = 60 °C (see discussion in section 2). Addition of more homopolymer causes the appearance of two mesophases, one of which is richer in homopolymer than the other. The two-mesophase region disappears with increasing ϕ_{HB}^0 and is replaced by a narrow single-mesophase region. Increasing the concentration of polybutadiene then causes the homopolymer to separate out as the limit of solubility in the mesophase is reached. Finally, when $\phi_{HB}^0 \simeq 0.9$, the concentration of homopolymer in the A and B regions of the mesophase is so high that the reduction in the free energy from having an ordered phase with separated blocks vanishes and the system becomes homogeneous. Figure 4, with T = 80 °C, shows a similar behavior to that in Figure 3 except that the additional minimum in the free energy has disappeared, along with the corresponding two-mesophase region on the diagram. The separation into two ordered phases for $T \ll T_C$ is clearly an enthalpic effect, originating from the large value of the χ_{AB} parameters. When one mesophase can no longer solubilize homopolymer in this case, a second homopolymer-rich mesophase forms. Increasing the homopolymer concentration beyond $\phi_{HB}^0 \simeq 0.3$, however, leads to its expulsion into a separate homogeneous phase. Although the actual position of the binodals is uncertain for $T \simeq 60$ °C, we believe that the prediction of two ordered mesophases is probably reliable because the incipient formation of the second minimum in the free energy is already evident at T = 80 °C, signalled by negative curvature in the free energy near $\phi_{HB}^0 \simeq 0.3$. However, the free energy in this region lies above the tangent joining the two binodal points shown so that these additional features are not stable at this temperature. For $T > T_C$ the interaction parameter χ_{AB} becomes too small to sustain a mesophase (Figure 5), and separation into two homogeneous phases occurs. For $T \gg T_C$ the system remains homogeneous (Figure 6).

Next we consider the effects of varying the molecular weight of the homopolymer. Figures 7–12 show the result of increasing the molecular weight of the butadiene homopolymer by almost an order of magnitude. Fixing the temperature at T = 80 °C, for example, we see that the system remains homogeneous until $Z_{HB} > 50$, at which point induced mesophase formation sets in. The weight fraction of homopolymer that can be solubilized in the mesophase at a fixed temperature then decreases rapidly as Z_{HB} increases (Figures 10 and 11), until for $Z_{HB} \simeq 150$ the system begins to separate into two homogeneous phases. Note that Figure 11 corresponds to Figures 3–6 except that the amount of homopolymer in Figure 11 is measured in terms of the weight fraction of polybutadiene instead of the volume fraction. The two diagrams are very similar, however, since the nonlinearity in converting from the one measure of the amount of butadiene homopolymer to the other is small in this case.

Figure 9 shows a type of critical point, corresponding to the minimum value of χ_{PS-PBD} on the spinodal curve, that was not present in Figure 3. The free-energy curves

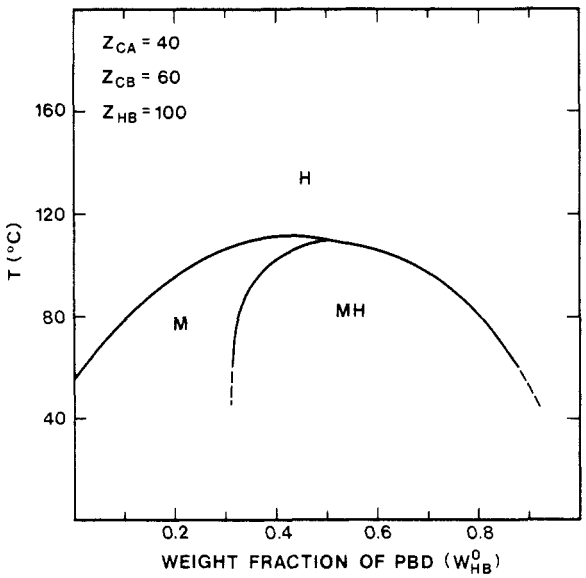

Figure 10. Phase diagram for a blend of polybutadiene homopolymer with styrene–butadiene block copolymer, as in Figure 9, but with an increased degree of polymerization for the butadiene homopolymer.

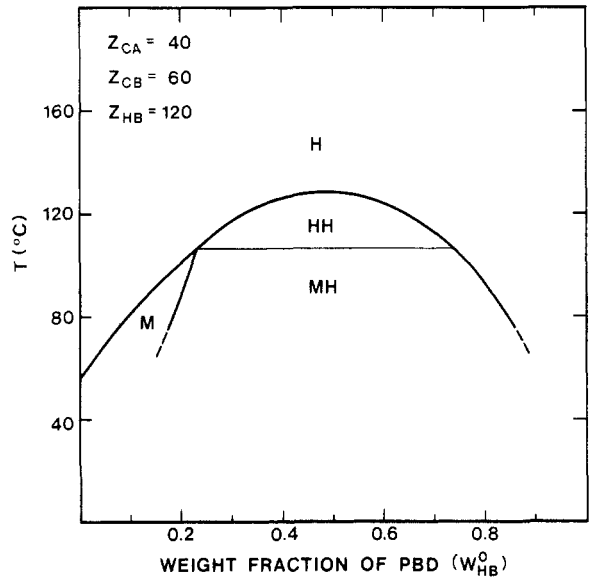

Figure 11. Phase diagram for a blend of polybutadiene homopolymer with styrene–butadiene block copolymer, as in Figure 10, but with an increased degree of polymerization for the butadiene homopolymer.

corresponding to cuts across the diagram for different temperatures are shown in Figures 13–15. As previously, we denote the temperature at which $\phi^* = \phi_1 (=\phi_2)$ by T_C. For $T < T_C$, the inhomogeneous free energy vanishes for $\phi > \phi^*$ in this case. For $\phi < \phi^*$, the total free energy in the vicinity of the left binodal point ϕ_1 is then given by eq 3-11, with the corresponding expression in the vicinity of the right binodal point $\phi_2 > \phi^*$ given by eq 3-12. Above T_C the boundary between the homogeneous and mesophase is just $\phi = \phi^*(T)$. Using equation 3-7, we find for $T \lesssim T_C$, i.e., $\phi_1 \lesssim \phi^* \lesssim \phi_2$

$$\lim_{T\to T_C^-} \frac{\delta\phi_2}{\delta T} = -\frac{\epsilon}{\tilde{C}(\phi_2 T_C)} \lim_{T\to T_C^-} \left[\frac{\phi_1 - \phi^*}{\phi_2 - \phi_1} \left(\frac{\partial \phi^*}{\partial T} \right) \right] \quad (3\text{-}16)$$

and similarly

$$\lim_{T\to T_C^-} \frac{\delta\phi_1}{\delta T} = -\frac{\epsilon}{\tilde{C}(\phi_1 T_C)} \lim_{T\to T_C^-} \left[\frac{\phi_2 - \phi^*}{\phi_1 - \phi_2} \left(\frac{\partial \phi^*}{\partial T} \right) \right] \quad (3\text{-}17)$$

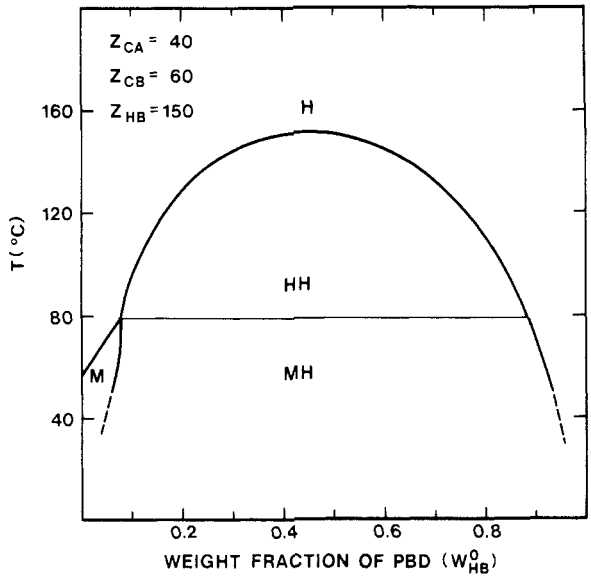

Figure 12. Phase diagram for a blend of polybutadiene homopolymer with styrene–butadiene block copolymer, as in Figure 11, but with an increased degree of polymerization for the butadiene homopolymer.

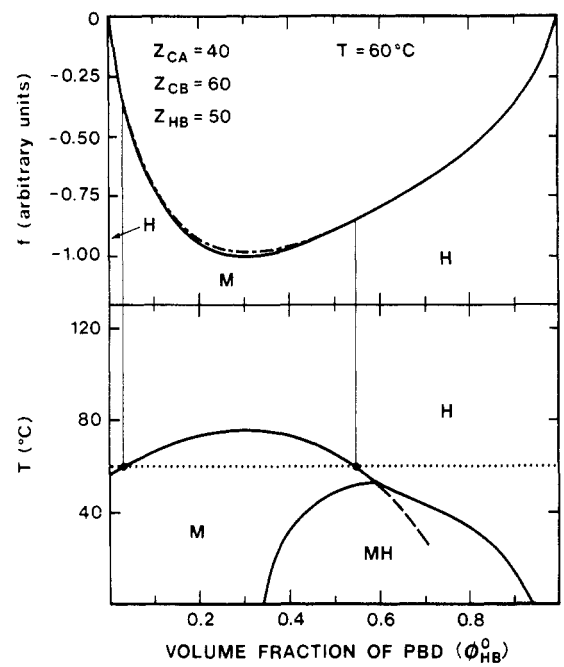

Figure 13. Phase diagram for styrene–butadiene block copolymer blended with polybutadiene homopolymer for the degrees of polymerization of the different components as marked on the diagram. The subscript A refers to polystyrene, and B to polybutadiene. The free-energy curves for $T = 60$ °C are shown. The dot–dash line shows the homogeneous free energy, and the solid line corresponds to the total free energy, including the inhomogeneous part. Different regions of the diagram are labeled H (homogeneous), M (mesophase), and MH (mesophase–homogeneous). The solid vertical lines correspond to the critical values of $\phi_{HB}{}^0$ (called ϕ^* in the text) at which the inhomogeneous free-energy term becomes negative. If at this point the curvature of the *total* free energy becomes negative, ϕ^* is one of the spinodal points inside the two-phase MH region. The corresponding spinodal trajectory is shown by the dashed line in the phase diagram. Note that this diagram, which is given in terms of the volume fraction of polybutadiene, is the basis for Figure 9, which shows the same figure, expressed in terms of the weight fraction of polybutadiene.

We take the limit by equating the slopes of the binodals at ϕ_1 and ϕ_2

$$\tilde{B}(\phi_1, T) - \epsilon(T)(\phi_1 - \phi^*) = \tilde{B}(\phi_2, T_C) \quad (3\text{-}18)$$

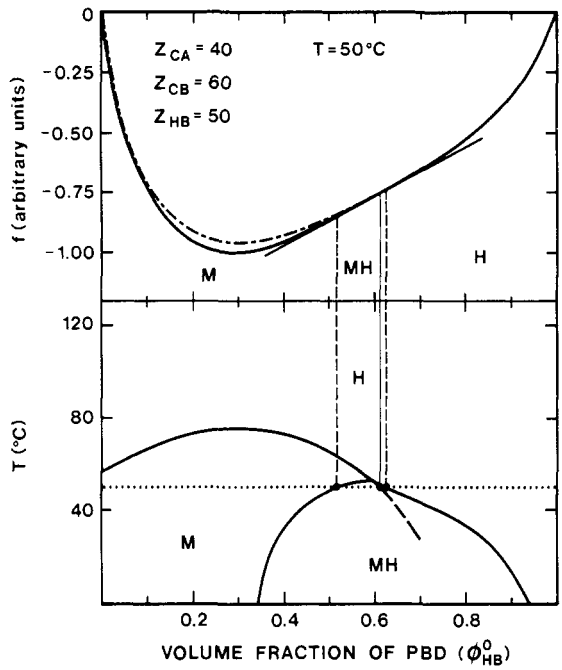

Figure 14. Same diagram as Figure 13, showing the free-energy curves and binodal constructions for T = 50 °C.

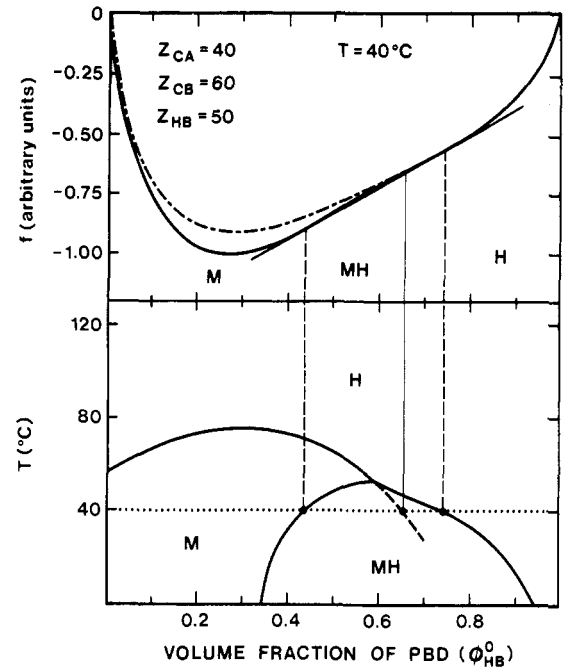

Figure 15. Same diagram as Figure 13, showing the free-energy curves and binodal constructions for T = 40 °C.

and by using eq 3-2, which derives from the binodal points being joined by a single line

$$\tilde{A}(\phi_2,T) - \tilde{A}(\phi_1,T) + \frac{\epsilon(T)}{2}(\phi_1 - \phi^*) = \tilde{B}(\phi_2,T)(\phi_2 - \phi_1) \tag{3-19}$$

Expanding the coefficients $\tilde{A}(\phi_2,T)$ and $\tilde{B}(\phi_2,T)$ about ϕ_1 and using the above relations, we find

$$\lim_{T\to T_C^-} \frac{\phi_1 - \phi^*}{\phi_2 - \phi_1} = 1 \tag{3-20}$$

so that eq 3-16 and 3-17 reduce to

$$\lim_{T\to T_C^-} \frac{\delta\phi_2}{\delta T} = \frac{\partial\phi^*}{\partial T} \tag{3-21}$$

and

$$\lim_{T\to T_C^-} \frac{\delta\phi_1}{\delta T} = 0 \tag{3-22}$$

Figure 13 clearly shows this behavior at the critical point ($T_C \simeq 53$ °C). Above T_C there is no phase separation, since the free-energy curve is concave upward everywhere, as shown in Figure 13 for T = 60 °C. However, the inhomogeneous free energy is negative between the two critical values of the homopolymer volume fraction marked by the vertical lines. For $T > T_C$ the locus of these points forms the spinodal of the system with respect to microphase separation. When $T \lesssim T_C$, the magnitude of the coefficient $\epsilon(T)$ (eq 3-9) becomes large enough to change the sign of the curvature in the total free energy at the right-hand critical point (ϕ^*) for microphase formation, giving rise to two binodal points with $\phi_1 < \phi^* < \phi_2$. This situation is shown in Figure 14 for T = 50 °C. The dashed line on the phase diagram below T_C corresponds to the continuation of the spinodal for microphase formation into the region where the phase separation into the ordered and homogeneous phases takes place. The other spinodal line, which terminates at T_C, is not shown. Note that the free energy (solid line) does not go to 0 for $\phi_{HB}{}^0 = 0$ at the left-hand side of the free energy diagram, indicating that the ordered phase of the pure block copolymer system is more stable than the homogeneous phase. As a consequence, the spinodal for microphase separation at $\phi_{HB}{}^0 = 0$ lies *above* T = 50 °C (dotted line) on the phase diagram. Figure 15 shows the widening of the MH region as the inhomogeneous free energy gets larger with decreasing temperature. Specifically, the magnitude of the coefficient $\epsilon(T)$ becomes larger with a drop in temperature, causing a bigger change in the curvature of the free energy at ϕ^*; the larger Δf then broadens the region over which separation into a mesophase and a homogeneous phase takes place.

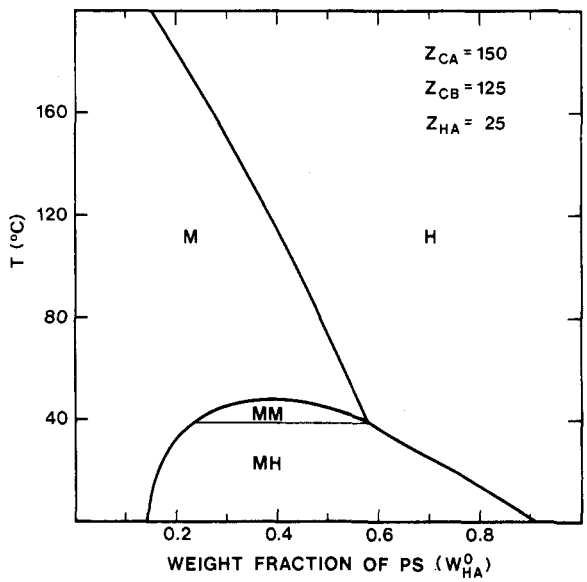

Figure 16. Phase diagram for a blend of polystyrene homopolymer with styrene–butadiene block copolymer for the degrees of polymerization of the different components as indicated on the figure. The subscript A refers to polystyrene, and B to polybutadiene. Note that the amount of polystyrene is measured in terms of the weight fraction ($W_{HA}{}^0$).

Figures 16 and 17 show the phase diagrams of a block copolymer–homopolymer system with larger degrees of polymerization for the polystyrene and polybutadiene blocks than in the earlier figures. The interesting feature of these diagrams, which shows up for small homopolymer molecular weight, is the occurrence of a small MM (mesophase–mesophase) region near the eutectic point where

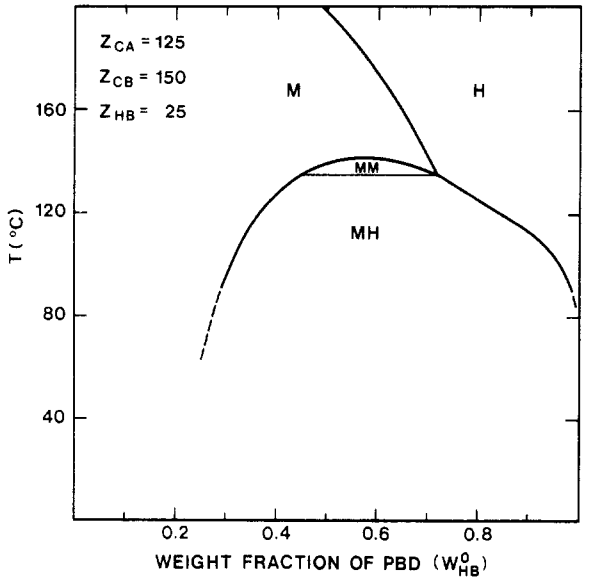

Figure 17. Phase diagram for a blend of polybutadiene homopolymer with styrene–butadiene block copolymer for the degrees of polymerization of the different components as indicated on the figure. The subscript A refers to polystyrene, and B to polybutadiene. Note that the amount of polybutadiene is measured in terms of the weight fraction (W_{HB}^0).

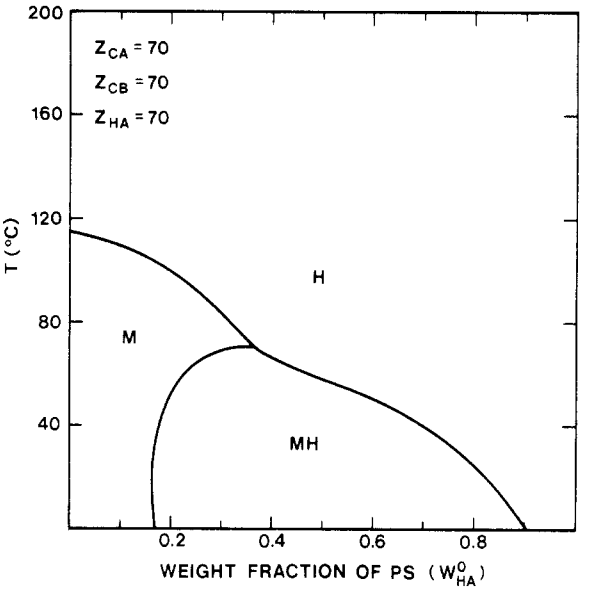

Figure 18. Phase diagram for a blend of polystyrene homopolymer with styrene–butadiene block copolymer for the degrees of polymerization of the different components as indicated on the figure. The subscript A refers to polystyrene, and B to polybutadiene. Note that the amount of polystyrene is measured in terms of the weight fraction (W_{HA}^0).

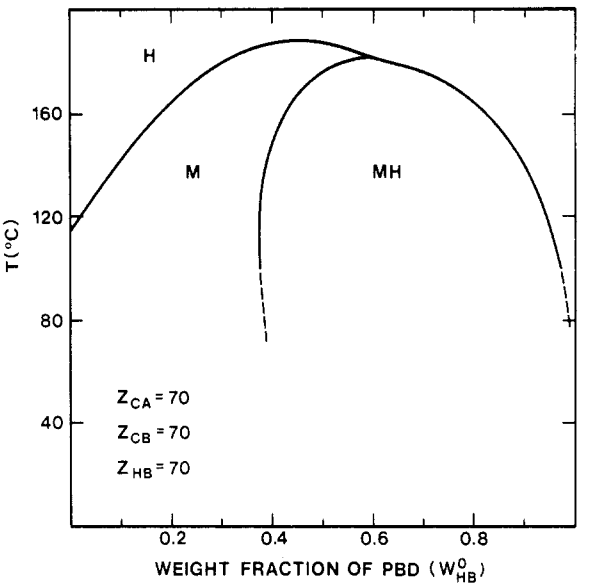

Figure 19. Phase diagram for a blend of polybutadiene homopolymer with styrene–butadiene block copolymer for the degrees of polymerization of the different components as indicated on the figure. The subscript A refers to polystyrene, and B to polybutadiene. Note that the amount of polybutadiene is measured in terms of the weight fraction (W_{HB}^0).

two mesophases and the homogeneous phase are in equilibrium (see also Figure 8). This structure arises from a small double minimum in the free energy similar to the one displayed in Figure 3. Aside from the transition from MM and M into an MH region in Figure 3 (because of the binodal point on the right-hand side of the diagram), as opposed to the transition from MM and M into the H region in Figure 16, the free-energy curves and binodal constructions are qualitatively similar for the corresponding temperature ranges in the two diagrams. Figures 16 and 17 differ only in the interchange of the degrees of polymerization of the sytrene and butadiene blocks, as well as the interchange of the polystyrene and polybutadiene homopolymer with the same degree of polymerization. However, the difference in the density and the molecular weight of the two materials is sufficient to shift the diagram features by nearly 100 °C.

An even more drastic effect on the phase diagram from changing the homopolymer is seen in Figures 18 and 19. Here all the degrees of polymerization remain the same, but the homopolymer is changed from polystyrene in Figure 18 to polybutadiene in Figure 19. Aside from the shift in the diagram on the temperature scale, Figure 19 predicts induced mesophase formation with the addition of polybutadiene for high temperatures, whereas Figure 18 shows that the mesophase is likely to be dissolved by the addition of polystyrene over a considerable temperature range. These two diagrams give a vivid example that model calculations, such as shown in Figure 2, which assume equal densities for all components are of limited value and that even qualitative features may not survive when the material composition of the system is changed.

(c) Order of the Homogeneous-Phase–Mesophase Transition. Throughout this paper we have assumed that the microdomains have a lamellar structure, so that the third-order terms in the expansion of the free energy in terms of the variations of the densities about their average values vanishes. Leibler has shown that this is not strictly true for pure asymmetric block copolymer with $f_A \neq f_B$, and the expansion of the free energy then contains a third-order term, which allows for the formation of additional periodic microdomain structures that are not lamellar.[14] According to Landau's theory of phase transitions, the transition between the homogeneous phase and the mesophase is first order in this case.[26] In our model, however, the inhomogeneous free energy, eq 3-9, has a quadratic expansion about the critical value of the homopolymer volume fraction ϕ^*. Thus the derivative $\partial\Delta f/\partial\phi$ vanishes at $\phi = \phi^*$, and the transition is in general second order for a small inhomogeneous free-energy contribution, provided the effect of thermal fluctuations is ignored.[26] As discussed in section 2b, when the magnitude of the inhomogeneous term grows, the second derivative $\epsilon(T) = -\partial^2\Delta f/\partial\phi^2$ at $\phi = \phi^*$ can become large enough to cause a change in the sign of the curvature of the total free energy at this point and we obtain a two-phase region between the homogeneous phase and the mesophase. The occur-

rence of a second-order transition between the M and H phases for certain parts of the phase diagram is strictly due to our assumption of a lamellar mesophase and may be replaced by a first-order transition in a more general treatment that allows other morphologies for asymmetric block copolymers with selective solvents.

4. Discussion

One important result that derives from the calculated phase diagrams, in particular the series shown in Figures 7–12, is the solubility of the homopolymer in the block copolymer microdomains as a function of the homopolymer chain length. For a given temperature, $T \simeq 70$ °C for example, Figure 7 shows that no mesophase formation takes place for small polybutadiene chain length, $Z_{HB} = 20$. Increasing the degree of polymerization of the homopolymer to $Z_{HB} = 50$ (Figure 9) leads to induced mesophase formation and eventual dissolution of the ordered phase as the weight fraction of polybutadiene is increased. For lower temperatures, a two-phase region appears, as the limit of solubility of the homopolymer in the mesophase is reached. Depending on the temperature, about 30% w/w of polybutadiene can be dissolved in the block copolymer microstructure. Increasing the molecular weight of the homopolymer leads to a rapid drop in the solubility, as is evident from Figures 11 and 12, reflecting the difficulty of accommodating high molecular weight homopolymer in a confined domain structure. These results are in qualitative agreement with recent experiments by Roe and Zin[1,2] that show similar trends, although their microdomains were most likely spherical and not lamellar. An earlier theory by Meier[27] gives much smaller solubilities of homopolymer in the block copolymer microdomains.

Another interesting result of the theory is the topological similarity of some of our diagrams, in particular Figure 3, with those derived from the recent experiments by Roe and Zin.[1,2] Again, detailed comparison is difficult because the copolymer block lengths for Roe's material were compatible with a spherical microdomain structure, but a remarkable similarity exists between his Figure 7 and our Figure 3, even to the point of predicting two mesophases at low temperature. A notable difference is the existence of two close binodal lines between the homogeneous and mesophase regions for small homopolymer weight fraction in the experimental diagram, terminating at the eutectic temperature. The theoretical calculation shows a coalescence of the two binodals into a single line terminating at a single eutectic point. As discussed in section 3, this is due to our restriction to a lamellar mesophase, which results in a second-order transition between the ordered and homogeneous phases.

In general, multiplying all the chain lengths by the same factor just shifts the phase diagrams up or down the temperature scale consistent with the same values of χZ. Clearly a more general way of presenting the theoretical results is to fix the ratios of the molecular weights and to plot χZ for one of the components vs. homopolymer volume or weight fraction. However, we have chosen to present our results in a less general way for the specific system of polystyrene or polybutadiene mixed with styrene–butadiene copolymer in order to make the main features more accessible to experimental comparison. The calculations for other materials and different temperature ranges can easily be carried out by using the computer code that is available as supplementary material to this paper. It should be emphasized again that so far the theoretical phase diagram calculations are available only for a lamellar structure.

We have shown how to calculate the equilibrium phase diagrams for a block copolymer–homopolymer blend. The theory also gives the density profiles and periodicity of the ordered phase, a point we have not emphasized in the present paper. In spite of the many simplifying assumptions introduced in the theory, the way seems clear for more realistic treatments. For example, full self-consistent calculations can be carried out, eliminating the need for the one wavevector random-phase approximation. Free-volume effects can be incorporated quite easily,[18] and more detailed information about the interaction parameters and the densities of the pure materials can be included. Polydispersity effects can be accounted for,[28] and the theory can be extended to include varying degrees of randomness in the copolymer.[15] The phase diagrams including cylindrical and spherical morphologies for block copolymer–homopolymer blends will be the subject of another paper in this series.

As always, the impetus for carrying out more detailed theoretical work and elucidating the physical basis of new phenomena (such as homopolymer-induced microphase formation) must come from a systematic experimental study of block copolymer–homopolymer blends.

Acknowledgment. M. D. Whitmore wishes to thank the Natural Sciences and Engineering Research Council of Canada for the award of a Senior Industrial Fellowship and the Xerox Research Centre of Canada for hospitality during the course of this work.

Registry No. (Styrene)-(butadiene) (copolymer), 9003-55-8; polystyrene (homopolymer), 9003-53-6; polybutadiene (homopolymer), 9003-17-2.

Supplementary Material Available: Computer program for evaluating phase diagrams (15 pages). Ordering information is given on any current masthead page.

References and Notes

(1) Zin, W.-C.; Roe, R.-J. *Macromolecules* **1984**, *17*, 183.
(2) Roe, R.-J.; Zin, W.-C. *Macromolecules* **1984**, *17*, 189.
(3) Hashimoto, T.; Shibayama, M.; Fujimura, M.; Kawai, H. In "Block Copolymers Science and Technology"; Meier, D. J., Ed.; MMI Press (Harwood Academic Publishers): New York, 1983.
(4) Bates, F. S.; Bair, H. E.; Hartney, M. A. *Macromolecules* **1984**, *17*, 1987.
(5) Rigby, D.; Roe, R.-J. *Macromolecules* **1984**, *17*, 1778.
(6) Gaillard, P.; Ossenbach-Sauter, M.; Reiss, G. *Makromol. Chem., Rapid Commun.* **1980**, *1*, 771.
(7) Hadziioannou, G.; Skoulios, A. *Macromolecules* **1982**, *15*, 267.
(8) Cohen, R. E.; Torradas, J. M. *Macromolecules* **1984**, *17*, 1101.
(9) Helfand, E.; Tagami, Y. *J. Chem. Phys.* **1972**, *56*, 3592.
(10) Helfand, E. *Macromolecules* **1975**, *8*, 552.
(11) Helfand, E.; Wasserman, Z. R. In "Developments in Block Copolymers"; Goodman, I., Ed.; Applied Science: London, 1982.
(12) Noolandi, J.; Hong, K. M. *Ferroelectrics* **1980**, *30*, 117.
(13) Noolandi, J.; Hong, K. M. *Macromolecules* **1984**, *17*, 1531.
(14) Leibler, L. *Macromolecules* **1980**, *13*, 1602.
(15) Hong, K. M.; Noolandi, J. *Macromolecules* **1984**, *16*, 1083.
(16) Hong, K. M.; Noolandi, J. *Macromolecules* **1981**, *14*, 727.
(17) Noolandi, J.; Hong, K. M. *Polym. Bull. (Berlin)* **1982**, *7*, 561.
(18) Hong, K. M.; Noolandi, J. *Macromolecules* **1981**, *14*, 1229.
(19) Flory, P. J. *Discuss. Faraday Soc.* **1970**, *49*, 7.
(20) Sanchez, I. C.; Lacombe, R. H. *Macromolecules* **1978**, *11*, 1145.
(21) Noolandi, J.; Hong, K. M. *Macromolecules* **1982**, *15*, 482.
(22) Gordon, P. "Principles of Phase Diagrams In Materials Systems"; McGraw-Hill: New York, 1968.
(23) Brandrup, J.; Immergut, E. H., Eds.; "Polymer Handbook"; Interscience: New York, 1966.
(24) Richardson, M. J.; Savill, N. G. *Polymer* **1977**, *18*, 3.
(25) Roe, R.-J.; Zin, W.-C. *Macromolecules* **1980**, *13*, 1221.
(26) Lifshitz, E. M.; Pitaevskii, L. P. "Statistical Physics by Landau and Lifshitz", 3rd ed.; Pergamon Press: New York, 1980; Part 1, Chapter 14. See also Alexander S.; Amit, D. J. *J. Phys. A: Math. Gen.* **1975**, *8*, 1988.
(27) Meier, D. J. *Polym. Prepr. (Am. Chem. Soc., Div. Polym. Chem.)* **1977**, *18*(1), 340.
(28) Solc, K.; Kleintjens, L. A.; Koningsveld, R. *Macromolecules* **1984**, *17*, 573.